

Hydrothermal Synthesis and Structural Characterization of a Novel Organic-Inorganic Hybrid Compound $\{[\text{Cu}(2, 2'\text{-bpy})_2]_2\text{-Mo}_8\text{O}_{26}\}$

WANG, Yong-Hui^a(王永慧) CHEN, Li-Dong^a(陈立东) HU, Chang-Wen^{*a}(胡长文)

WANG, En-Bo^a(王恩波) JIA, Heng-Qing^b(贾恒庆) HU, Ning-Hai^b(胡宁海)

^aInstitute of Polyoxometalate Chemistry, Faculty of Chemistry, Northeast Normal University, Changchun, Jilin 130024, China

^bChangchun Institute of Applied Chemistry, Chinese Academy of Sciences, Changchun, Jilin 130022, China

A novel organic-inorganic hybrid compound $\{[\text{Cu}(2, 2'\text{-bpy})_2]_2\text{-Mo}_8\text{O}_{26}\}$ has been hydrothermally synthesized and structurally characterized by single-crystal X-ray diffraction. The compound crystallizes in the orthorhombic space group, $Pna2_1$, with $a = 2.4164(5)$, $b = 1.8281(4)$, $c = 1.1877(2)$ nm, $V = 5.247(2)$ nm³, $Z = 4$, and final $R_1 = 0.0331$, $wR_2 = 0.0727$. The structure consists of discrete $\{[\text{Cu}(2, 2'\text{-bpy})_2]_2\text{-Mo}_8\text{O}_{26}\}$ clusters, constructed from a β -octamolybdate subunit $[\text{Mo}_8\text{O}_{26}]^{4-}$ covalently bonded to two $[\text{Cu}(2, 2'\text{-bpy})_2]^{2+}$ coordination complex cations via bridging oxo groups. In addition, the spectroscopic properties and thermal behavior of this compound have been investigated by spectroscopic techniques (UV-vis, IR, Raman and EPR spectra) and TG analysis.

Keywords organic-inorganic hybrid compound, octamolybdate, transition metal coordination complexes, hydrothermal synthesis, structural characterization

Introduction

Organic-inorganic hybrid materials consisting of organic and inorganic components, especially metal oxides, are of great interest because these materials can exhibit synergetic properties such as electrical, magnetic and optical properties.¹ Recently, a number of such materials constructed from metal-oxo clusters (polyoxometa-

lates, POMs) linked to transition metal coordination complexes have been prepared via hydrothermal synthesis,²⁻⁵ such as $[\text{M}(4, 4'\text{-bpy})(\text{VO}_2)_2(\text{HPO}_4)_4]$ ($\text{M} = \text{Co}, \text{Ni}$; bpy = bipyridine)₂ and $[\text{Ni}(2, 2'\text{-bpy})_3]_{1.5}[\text{PW}_{12}\text{O}_{40}\text{Ni}(2, 2'\text{-bpy})_2(\text{H}_2\text{O})] \cdot 0.5\text{H}_2\text{O}$.³ In this way, a series of novel organic-inorganic materials consisting of molybdenum-oxo clusters attached to various transition metal complexes have been reported and exhibited a rich structural chemistry.^{4,6-11} Typical examples include $\{\text{Mo}_3\text{O}_{12}[\text{Fe}(2, 2'\text{-bpy})_2]_2\} \cdot 0.25\text{H}_2\text{O}$,⁷ a 1-D chain, $[\{\text{Ni}(3, 3'\text{-bpy})_2\}_2\text{Mo}_4\text{O}_{14}]$,⁸ a 2-D layered network, $\{[\text{Ni}(2, 2'\text{-bpy})_2]_2\text{Mo}_4\text{O}_{14}\}$,⁹ which displays a simple ring structure, and $\{[\text{Fe}(\text{tpyr})]_3\text{Fe}(\text{Mo}_6\text{O}_{19})_2\} \cdot x\text{H}_2\text{O}$ ¹⁰ (tpyr = tetrapyritylporphyrin), which has a 3-D framework.

In addition, it is noteworthy that so far six isomers of the octamolybdate clusters, namely the α , β , γ , δ , ϵ , and ζ forms, have been described, whose structures differ in the number, type, and fusion mode of the molybdenum polyhedra.^{6,12-19} Furthermore, some organic-inorganic hybrid materials constructed from octamolybdates covalently bonded to various transition metal complexes have been hydrothermally synthesized.^{17,19-27} For example, $\{[\text{Ni}(4, 4'\text{-bpy})_2]_2(\text{H}_2\text{O})_2\text{Mo}_8\text{O}_{26}\}$ ²⁰ displays a 2-D network structure consisting of ϵ - $[\text{Mo}_8\text{O}_{26}]^{4-}$

* E-mail: huchw@nenu.edu.cn; Fax(Tel.): 0431-5640694.

Received April 3, 2001; revised July 9, 2001; accepted August 27, 2001.

Project supported by the National Natural Science Foundation of China (No. 20071007) and the Foundation for University Key Teacher by the Ministry of Education of China.

linked to 1-D $[\text{Ni}(4,4'\text{-bpy})_2]^{2+}$ chains. However, all of these octamolybdate isomers are linked with transition metal complexes through terminal oxo groups (thus acting as μ_2 -oxo bridges).

Here, we report the hydrothermal synthesis and structure characterization of a novel organic-inorganic hybrid compound $\{[\text{Cu}(2,2'\text{-bpy})_2]_2\text{Mo}_8\text{O}_{26}\}$. In its structure, a β -octamolybdate cluster covalently bonds to two $[\text{Cu}(2,2'\text{-bpy})_2]^{2+}$ coordination complexes *via* bridging oxo groups (thus serving as μ_3 -oxo bridges). Although in the chemistry of organometallic POMs the organometallic sites may be coordinated with the POM skeleton through terminal and/or bridging oxygen atoms,²⁸ which is perhaps a common feature, the unusual linking fashion in this case, to the best of our knowledge, is unique in the coordination chemistry of octamolybdates with transition metal complexes and even in that of the whole molybdenum-oxo clusters.

Experimental

General procedures

All chemicals were of analytical grade and used as obtained without further purification. Elemental analyses (C, H and N) were performed on a Perkin-Elmer 2400 CHN Elemental Analyzer. Mo and Cu were determined using a Leeman inductively coupled plasma atomic emission spectroscopy (ICP-AES). Diffuse reflectance UV-vis spectrum (BaSO_4 pellet) was obtained with a Varian Cary 500 UV-Vis-NIR spectroscopy. IR spectrum (KBr pellet) was recorded on an Alpha Centaur FT/IR spectrophotometer in the range 400–4000 cm^{-1} . Raman spectrum was recorded on a JY-UV-micro-laser Raman spectrometer using an argon laser (488 nm, ~50 mW). Thermogravimetric (TG) analysis was performed on a Perkin-Elmer TGA-7 thermal analyzer at a heating rate of 20 $^\circ\text{C}/\text{min}$ in flowing nitrogen atmosphere in the temperature range 30–730 $^\circ\text{C}$. EPR spectrum was recorded on a Japanese JES-FE3AX spectrometer at 293 K.

Hydrothermal synthesis

The title compound was hydrothermally synthesized under autogenous pressure. A mixture of $\text{CuCl}_2 \cdot 2\text{H}_2\text{O}$ (0.0341 g), *p*-phthalic acid (0.0338 g), 2,2'-bipyridine (0.0313 g), MoO_3 (0.0866 g), NaOH (0.0145

g) and H_2O (10 mL) in a molar ratio 1:1:1:3:1.8:2780 was sealed in a 20-mL Teflon-lined stainless steel autoclave and heated at 180 $^\circ\text{C}$ for 5 d. After cooling to room temperature, dark green block crystals were isolated by filtration and washed with distilled water (9.2% yield based on Mo). Anal. calc for $\text{C}_{40}\text{H}_{32}\text{Cu}_2\text{Mo}_8\text{N}_8\text{O}_{26}$: C 24.80, H 1.65, N 5.79, Cu 6.57, Mo 39.66; found C 24.92, H 1.70, N 5.85, Cu 6.41, Mo 39.87.

Single crystal X-ray diffraction

A dark green single crystal with dimensions 0.52 mm \times 0.40 mm \times 0.32 mm was mounted inside a glass fiber capillary. Diffraction data were collected at room temperature on a Siemens P4 four-circle diffractometer using graphite-monochromated Mo- $\text{K}\alpha$ radiation ($\lambda = 0.071073$ nm) using the ω -scan technique. Details of crystal data and structure refinement are listed in Table 1.

Table 1 Crystal data and structure refinement for $\{[\text{Cu}(2,2'\text{-bpy})_2]_2\text{Mo}_8\text{O}_{26}\}$

Molecular formula	$\text{C}_{40}\text{H}_{32}\text{Cu}_2\text{Mo}_8\text{N}_8\text{O}_{26}$
Formula weight	1935.34
Crystal system	orthorhombic
Space group	$Pna2_1$
<i>a</i> (nm)	2.4164(5)
<i>b</i> (nm)	1.8281(4)
<i>c</i> (nm)	1.1877(2)
<i>V</i> (nm^3)	5.247(2)
<i>Z</i>	4
λ (Mo $\text{K}\alpha$) (nm)	0.071073
<i>T</i> (K)	293(2)
ρ (g/cm^3)	2.450
<i>F</i> (000)	3720
μ (Mo $\text{K}\alpha$) (mm^{-1})	2.733
Reflections collected	6193
Independent reflections	5353 ($R_{\text{int}} = 0.0186$)
Final R indices [$I > 2\sigma(I)$]	$R_1 = 0.0331$, $wR_2 = 0.0727$
R indices (all data)	$R_1 = 0.0422$, $wR_2 = 0.0749$
Goodness of fit	1.016

A total of 6193 reflections were measured in the range $1.69^\circ < \theta < 25.04^\circ$. A total of 5353 reflections were independent, applying the criterion $I > 2\sigma(I)$. A semi-empirical absorption correction (PSI SCAN) was applied for selected reflections. The structure was solved

by direct methods and refined by the Full-matrix least-squares on F^2 using the SHELXL-93 computer program. All non-hydrogen atoms were refined anisotropically. Hydrogen atoms were located from difference Fourier

maps. The final R factors were $R_1 = 0.0331$ [$wR_2 = 0.0727$] $\{R_1 = \sum \|F_o| - |F_c| \| / \sum |F_o|$; $wR_2 = \sum [w(F_o^2 - F_c^2)^2] / \sum [w(F_o^2)^2]^{1/2}\}$. Selected bond lengths and angles are given in Table 2.

Table 2 Selected bond lengths (nm) and angles ($^\circ$) of $\{[\text{Cu}(2,2'\text{-bpy})_2]_2\text{Mo}_8\text{O}_{26}\}$.

Bond distance (nm)					
Mo(1)—O(6)	0.1675 (8)	Mo(1)—O(5)	0.1690(9)	Mo(1)—O(2)	0.1938 (6)
Mo(1)—O(3)	0.1979 (7)	Mo(1)—O(1)	0.2285 (7)	Mo(1)—O(4)	0.2390 (6)
Mo(2)—O(10)	0.1675(8)	Mo(2)—O(9)	0.1680(8)	Mo(2)—O(7)	0.1902(7)
Mo(2)—O(2)	0.1967(7)	Mo(2)—O(8)	0.2310(7)	Mo(2)—O(1)	0.2482(7)
Mo(3)—O(13)	0.1691(8)	Mo(3)—O(12)	0.1692(8)	Mo(3)—O(7)	0.1887(7)
Mo(3)—O(11)	0.1996(6)	Mo(3)—O(14)	0.2326(7)	Mo(3)—O(1)	0.2338(7)
Mo(4)—O(15)	0.1677(7)	Mo(4)—O(16)	0.1746(7)	Mo(4)—O(11)	0.1693(6)
Mo(4)—O(3)	0.1951(8)	Mo(4)—O(1)	0.2158(7)	Mo(4)—O(17)	0.2342(6)
Mo(5)—O(20)	0.1688(7)	Mo(5)—O(19)	0.1699(7)	Mo(5)—O(18)	0.1893(7)
Mo(5)—O(4)	0.1973(6)	Mo(5)—O(3)	0.2332(7)	Mo(5)—O(17)	0.2354(7)
Mo(6)—O(21)	0.1688(7)	Mo(6)—O(8)	0.1720(7)	Mo(6)—O(4)	0.1927(7)
Mo(6)—O(14)	0.1952(7)	Mo(6)—O(17)	0.2175(7)	Mo(6)—O(1)	0.2361(7)
Mo(7)—O(24)	0.1685(8)	Mo(7)—O(23)	0.1706(8)	Mo(7)—O(22)	0.1930(6)
Mo(7)—O(14)	0.1993(7)	Mo(7)—O(17)	0.2274(7)	Mo(7)—O(11)	0.2349(6)
Mo(8)—O(26)	0.1675(8)	Mo(8)—O(25)	0.1701(7)	Mo(8)—O(18)	0.1915(8)
Mo(8)—O(22)	0.2441(7)	Mo(8)—O(16)	0.2267(7)	Mo(8)—O(17)	0.1960(7)
Cu(1)—N(21)	0.1968(8)	Cu(1)—N(12)	0.1973(8)	Cu(1)—N(22)	0.2028(9)
Cu(1)—N(11)	0.2046(9)	Cu(1)—O(2)	0.2221(8)	Cu(2)—N(42)	0.1963(8)
Cu(2)—N(31)	0.1964(8)	Cu(2)—N(41)	0.2017(8)	Cu(2)—N(32)	0.2052(10)
Cu(2)—O(22)	0.2244(8)				
Bond angle ($^\circ$)					
Mo(1)-O(2)-Mo(2)	115.7(4)	Mo(1)-O(2)-Cu(1)		114.7(3)	
Mo(2)-O(2)-Cu(1)	125.4(3)	Mo(7)-O(22)-Mo(8)		114.7(4)	
Mo(7)-O(22)-Cu(2)	122.8(3)	Mo(8)-O(22)-Cu(2)		119.0(10)	
N(21)-Cu(1)-N(12)	174.1(4)	N(21)-Cu(1)-N(22)		81.4(4)	
N(12)-Cu(1)-N(22)	97.7(4)	N(21)-Cu(1)-N(11)		103.3(3)	
N(12)-Cu(1)-N(11)	81.8(3)	N(22)-Cu(1)-N(11)		130.0(4)	
N(21)-Cu(1)-O(2)	92.4(3)	N(12)-Cu(1)-O(2)		83.1(3)	
N(22)-Cu(1)-O(2)	122.2(3)	N(11)-Cu(1)-O(2)		107.5(3)	
N(42)-Cu(2)-N(31)	172.9(4)	N(42)-Cu(2)-N(41)		82.5(3)	
N(31)-Cu(2)-N(41)	100.7(3)	N(42)-Cu(2)-N(32)		100.3(4)	
N(31)-Cu(2)-N(32)	82.1(4)	N(41)-Cu(2)-N(32)		133.4(4)	
N(42)-Cu(2)-O(22)	85.0(3)	N(31)-Cu(2)-O(22)		87.9(3)	
N(41)-Cu(2)-O(22)	113.9(3)	N(32)-Cu(2)-O(22)		112.7(3)	

Results and discussion

Synthesis

The original intent to introduce *p*-phthalic acid into the reaction system was to obtain a novel organic-inor-

ganic hybrid compound containing mixed organic ligands including *p*-phthalic acid and 2,2'-bipyridine. However, the obtained title compound contains no *p*-phthalic acid ligands but only 2,2'-bipyridine. Moreover, an interesting phenomenon was observed, that is, only when *p*-phthalic acid was introduced into the reaction system

could the title compound be obtained. Several control experiments without the addition of *p*-phthalic acid have been performed under the same synthetic conditions, but the outcome did not contain this compound at all. It is assumed that *p*-phthalic acid probably play double roles during the process. On the one hand, owing to its acidic nature, it may adjust the acidity of the reaction medium since the pH value of the medium after hydrothermal reaction is about 3.7 at which the β -[Mo₈O₂₆]⁴⁻ cluster can exist stably.³¹ On the other hand, it maybe acts as a template in the formation of the title compound. Study on this respect is still underway. Furthermore, the appropriate concentration of NaOH is essential to the formation of the title compound. The highest yield occurs when the NaOH concentration is 0.036 mol/L, while at other concentrations the yield is far lower and even the title compound does not exist.

Crystal structure

Fig. 1 displays the structure of $\{[\text{Cu}(2,2'\text{-bpy})_2]_2\text{Mo}_8\text{O}_{26}\}$ showing atom-labeling schemes and the 50% probability displacement ellipsoids. As shown, the crystal structure of the title compound consists of discrete $\{[\text{Cu}(2,2'\text{-bpy})_2]_2\text{Mo}_8\text{O}_{26}\}$ clusters, constructed from the β -octamolybdate subunit [Mo₈O₂₆]⁴⁻ covalently

linked to two [Cu(2,2'-bpy)₂]²⁺ coordination cations. A remarkable structural feature of this compound is the presence of an unusual bonding fashion between the molybdenum-oxo cluster and the copper coordination complexes, namely the β -[Mo₈O₂₆]⁴⁻ cluster bonds to the [Cu(2,2'-bpy)₂]²⁺ cations *via* bridging oxo groups that connect two adjacent molybdenum sites (thus serving as μ_3 -oxo bridges). The [Mo₈O₂₆]⁴⁻ moiety is composed of eight edge-sharing {MoO₆} octahedra and displays the characteristic β -octamolybdate arrangement, in which two Mo₄O₁₃ subunits are stacked together by relatively long Mo—O bonds.²⁹ All molybdenum sites exhibit +VI oxidation state and are crystallographically independent, possessing octahedral coordination geometry with different distortion extents. The Mo—O bonds can be divided into four groups: (i) Mo—O(*t*) bonds, 0.1675(8)—0.1706(8) nm; (ii) Mo—O(μ_2) bonds, 0.1720(7)—0.2310(7) nm; (iii) Mo—O(μ_3) bonds, 0.1925(6)—0.2390(6) nm; and (iv) Mo—O(μ_5) bonds, 0.2158(7)—0.2482(7) nm. The +VI oxidation state is also confirmed by bond valence sum calculations. The empirical bond valence calculation, $S = \exp(1.907 - R)/0.37$ (S = bond valence, R = bond length), leads to S values for Mo(1), Mo(2), Mo(3), Mo(4), Mo(5), Mo(6), Mo(7) and Mo(8) of 6.044, 6.131, 6.057, 6.044, 6.053, 6.076, 5.950 and 6.076, re-

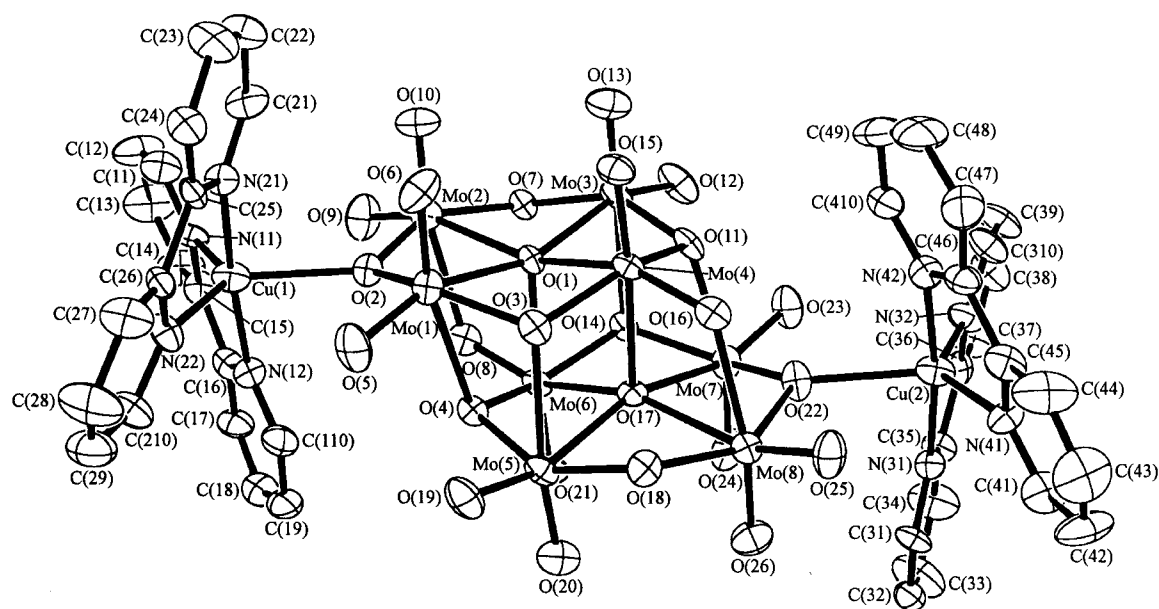


Fig. 1 Structure of $\{[\text{Cu}(2,2'\text{-bpy})_2]_2\text{Mo}_8\text{O}_{26}\}$ showing atom-labeling scheme and the 50% probability displacement ellipsoids. H atoms have been omitted for clarity.

spectively. The average value for the calculated oxidation states of Mo is 6.054, consistent with the formula of the title compound given by X-ray structure determination.

Each of the two copper coordination complex subunits, $[\text{Cu}(2,2'\text{-bpy})_2]^{2+}$, is covalently linked to the octamolybdate core via a double bridging oxo ligand ligated to two adjacent molybdenum centers (Fig. 1). The two bridging oxo ligands, O(2) and O(22), thus serve as μ_3 -oxo bridges. The bond distances of Mo(1)—O(2), Mo(2)—O(2), Mo(7)—O(22) and Mo(8)—O(22) are 0.1938(6), 0.1967(7), 0.1930(6) and 0.1960(7) nm, respectively. The copper (II) sites exhibit distorted square pyramidal $\{\text{CuN}_4\text{O}\}$ geometry. As shown in Fig. 1, each copper center is coordinated to four nitrogen donors of the 2,2'-bipyridine ligands at the basal plane and one bridging oxo group of the octamolybdate cluster at the apical position. The eight Cu—N bond distances range from 0.1963(8) to 0.2052(10) nm and the two Cu—O bond lengths are 0.2221(8) and 0.2244(8) nm. In fact, such a "4 + 1" square pyramidal geometry for Cu (II) is not uncommon, and has been observed in several compounds such as $[\text{Cu}(\text{pz})_{0.5}\text{MoO}_4]$,¹¹ $[\text{Cu}(o\text{-phen})\text{MoO}_4]$ ²⁴ and $\{[\text{Cu}(o\text{-phen})_2]_2\text{Mo}_8\text{O}_{26}\}$.²⁴ In the latter compound each copper site is coordinated with four nitrogen donors and a terminal oxo group from the $\alpha\text{-}[\text{Mo}_8\text{O}_{26}]^{4-}$ core with a Cu—O distance of 0.2192 nm.²⁴ Thus it can be seen that the Cu—O distances in $\{[\text{Cu}(2,2'\text{-bpy})_2]_2\text{Mo}_8\text{O}_{26}\}$ [0.2221(8) and 0.2244(8) nm] are slightly longer than that in $\{[\text{Cu}(o\text{-phen})_2]_2\text{Mo}_8\text{O}_{26}\}$, owing to the unusual coordination mode of the copper sites with the bridging oxo groups from the octamolybdate core. Moreover, among the four 2,2'-bipyridine ligands attached to the copper sites (1, 2, 3 and 4) 1 and 4 are nearly parallel with a dihedral of *ca.* 9.2°. So are 2 and 3 with a dihedral of *ca.* 7.8°. However, with respect to the two 2,2'-bipyridine ligands attached to the same copper site (1 and 2, 3 and 4), the dihedrals between them are *ca.* 45°.

Further, the title compound $\{[\text{Cu}(2,2'\text{-bpy})_2]_2\text{Mo}_8\text{O}_{26}\}$ does not form the expected 1-D chain, 2-D layer or 3-D structure, but exhibits a discrete cluster structure. The present structure is reminiscent of $[\text{Cu}(\text{phen})_2]_2\{[\text{Cu}(\text{phen})_2\text{Mo}_8\text{O}_{26}\} \cdot \text{H}_2\text{O}$ reported by Xu *et al.*,²⁶ which contains a centrometric β -octamolybdate-supported complex anions $\{[\text{Cu}(\text{phen})_2\text{Mo}_8\text{O}_{26}\}^{2-}$.

In addition, Zubieta *et al.* have also reported a β -octamolybdate-containing organic-inorganic composite solid, $[\{[\text{Ni}(2,2'\text{-bpy})_2]_2\text{Mo}_4\text{O}_{13}\}]$, in which the $\beta\text{-}[\text{Mo}_8\text{O}_{26}]^{4-}$ clusters are linked by $[\text{Ni}(2,2'\text{-bpy})_2]^{2+}$ bridges into a 1-D chain.²⁵ However, not only the $\beta\text{-}[\text{Mo}_8\text{O}_{26}]^{4-}$ clusters in these two compounds but also those octamolybdate clusters pertaining to different isomers in the afore mentioned organic-inorganic hybrid materials are all linked with the transition metal complex cations via terminal oxo ligands from the octamolybdate core (thus acting as μ_2 -oxo bridges).¹⁸⁻²⁷ Therefore, to the best of our knowledge, the unique linking mode in this case, *i. e.*, the $\beta\text{-}[\text{Mo}_8\text{O}_{26}]^{4-}$ cluster bonds to the $[\text{Cu}(2,2'\text{-bpy})_2]^{2+}$ complexes *via* bridging oxo groups (thus acting as μ_3 -oxo bridges), represents the first example in the coordination chemistry of octamolybdates with transition metal complex fragments and even in that of the whole molybdenum-oxo clusters, except in the chemistry of organometallic POMs where the organometallic sites may be coordinated with the POM skeleton through terminal and/or bridging oxygen atoms. Further, it is noteworthy that from the same Cu-2,2'-bipyridine-Mo system several organic-inorganic hybrid materials containing molybdenum-oxo clusters have been prepared by hydrothermal method, such as $\{[\text{Cu}(2,2'\text{-bpy})\text{Mo}_2\text{O}_7]\}$, $\{[\text{Cu}(2,2'\text{-bpy})\text{Mo}_3\text{O}_{10}]\}$, and $\{[\text{Cu}(2,2'\text{-bpy})\text{Mo}_4\text{O}_{13}]\}$, all exhibiting 1-D chain structure, distinct from the discrete cluster structure in the present paper. This apparently demonstrates that small variations in the hydrothermal reaction conditions such as time, temperature, pH value and stoichiometry can have a deep influence on the reaction products.⁶

UV-vis, IR, Raman and EPR spectra

The diffuse reflectance UV-vis spectrum of the title compound exhibits four characteristic absorption peaks in the range 190—1200 nm. The two peaks at 253 and 309 nm are associated with two kinds of Mo—O LMCT bands,²⁶ while the other two wide bands around 623 and 867 nm partially overlap and are assigned to Cu—N and Cu—O LMCT bands,³⁰ respectively, leading to the dark green coloration of this compound.

In the IR spectrum of the title compound the feature bands concerned with coordinated 2,2'-bipyridine are at 1602s, 1575m, 1474s and 1446s cm^{-1} , and

bands at 945, 910, 849, 722, 667 and 551 cm^{-1} are attributed to the Mo = O and Mo—O—Mo vibrations of the β -octamolybdate.^{31,32} In addition, the fingerprint bands of 2, 2'-bipyridine and the Mo—O vibrations overlap in the low wavenumber region, making definite assignment of some bands in this region difficult.

The Raman spectroscopy of this compound has also been studied. This compound displays a number of Raman bands at 1587, 988, 815, 658, 461, 329, 273, 139 and 116 cm^{-1} in the range 100—2000 cm^{-1} . According to the literature,³¹ the β -octamolybdate possesses an inherent Raman line at 971 cm^{-1} , which is assigned to the asymmetric stretch of Mo = O. However, the Raman spectrum of this complex shows an intense band at 988 cm^{-1} pertaining to the asymmetric stretch of Mo = O, the shift of which is perhaps influenced by the coordination of the β -octamolybdate with the copper-2,2'-bipyridine complexes. In view of the same reason, the assignment of the other Raman bands is too difficult to be discussed here.

As shown in Fig. 2, the room-temperature EPR spectrum of the title compound exhibits a sharp and strong (225 G peak-to-peak) signal, giving $g_{\text{av}} = 2.0075$. This g -value is consistent with the presence of the copper (II) ions in this compound.

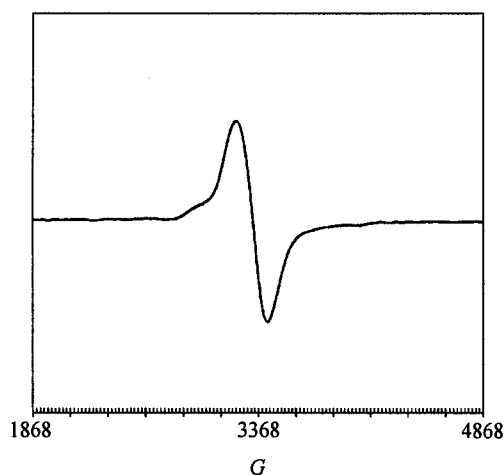


Fig. 2 EPR spectrum of $\{[\text{Cu}(2,2'\text{-bpy})_2]_2\text{Mo}_8\text{O}_{26}\}$.

TG analysis

The thermal behavior of the title compound has been investigated between 30 $^{\circ}\text{C}$ and 730 $^{\circ}\text{C}$. In the TGA curve this compound presents an approximate

three-step weight-loss process (Fig. 3). The first step in the temperature range *ca.* 295—380 $^{\circ}\text{C}$ corresponds to the loss of one 2,2'-bipyridine molecule on each copper site (calc. weight loss: 16.1%; found: 14.9%). The second step is between *ca.* 380 $^{\circ}\text{C}$ and 450 $^{\circ}\text{C}$ and corresponds to the loss of the remaining 2,2'-bipyridine molecules on copper centers (calc. weight loss: 16.1%; found: 15.4%). It can be observed that the result of the TG analysis basically agrees with that of the structure determination. The fact that the two 2,2'-bipyridine molecules bonding to the same copper site disassociate at different times perhaps results from the strength difference of the Cu—N bonds between the 2, 2'-bipyridine molecules and the copper sites. The exact mechanism on the loss of the four 2, 2'-bipyridine molecules needs further profound exploration. In the temperature range from 500 $^{\circ}\text{C}$ to 700 $^{\circ}\text{C}$ changes occur in the polyanion framework and the residue transforms into MoO_3 and CuO . The third step at temperatures higher than 700 $^{\circ}\text{C}$ is due to the evaporation of MoO_3 .

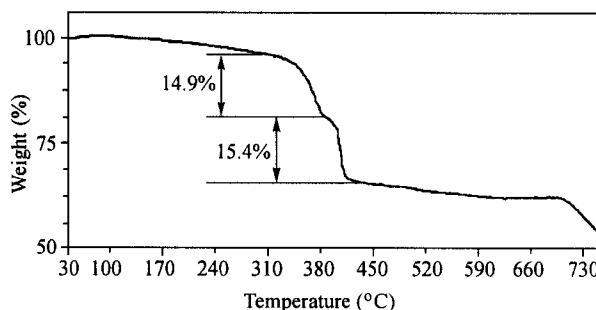


Fig. 3 TGA curve of $\{[\text{Cu}(2,2'\text{-bpy})_2]_2\text{Mo}_8\text{O}_{26}\}$.

Conclusion

We have successfully synthesized a novel organic-inorganic hybrid compound by the hydrothermal method. The structure of this compound consists of discrete $\{[\text{Cu}(2,2'\text{-bpy})_2]_2\text{Mo}_8\text{O}_{26}\}$ clusters, constructed from a β -octamolybdate subunit $[\text{Mo}_8\text{O}_{26}]^{4-}$ covalently bonded to two $[\text{Cu}(2,2'\text{-bpy})_2]^{2+}$ coordination complex cations via bridging oxo groups. The spectroscopic properties and thermal behavior of this compound have also been studied by UV-vis, IR, Raman, EPR spectra and TG analysis. The four 2,2'-bipyridine molecules in the title compound disassociate in two steps (295—380 $^{\circ}\text{C}$ and 380—450 $^{\circ}\text{C}$) and the β -octamolybdate skeleton begins to decompose at 500 $^{\circ}\text{C}$.

References

- 1 Kagan, C. R.; Mitzi, D. B.; Dimitrakopoulos, C. D. *Science* **1999**, *286*, 945.
- 2 Shi, Z.; Feng, S.-H.; Gao S.; Zhang, L.-R.; Yang, G.-Y.; Hua, J. *Angew. Chem., Int. Ed.* **2000**, *39*, 2325.
- 3 Xu, Y.; Xu, J.-Q.; Zhang, K.-L.; Zhang, Y.; You, X.-Z. *Chem. Commun.* **2000**, 153.
- 4 Hagrman, D.; Haushalter, R. C.; Zubieta, J. *Chem. Mater.* **1998**, *10*, 361.
- 5 Shi, Z.; Feng, S.-H.; Zhang, L.-R.; Yang, G.-Y.; Hua, J. *Chem. Mater.* **2000**, *12*, 2930.
- 6 Hagrman, P. J.; Hagrman, D.; Zubieta, J. *Angew. Chem., Int. Ed.* **1999**, *38*, 2638.
- 7 Zapf, P. J.; Hammond, R. P.; Haushalter, R. C.; Zubieta, J. *Chem. Mater.* **1998**, *10*, 1336.
- 8 Laduca, R. L. Jr.; Desciak, M.; Laskoski, M.; Rarig, R. S. Jr.; Zubieta, J. *J. Chem. Soc., Dalton Trans.* **2000**, 2255.
- 9 Zhang, Y.; Zapf, P. J.; Meyer, L. M.; Haushalter, R. C.; Zubieta, J. *Inorg. Chem.* **1997**, *36*, 2159.
- 10 Hagrman, D.; Hagrman, P. J.; Zubieta, J. *Angew. Chem., Int. Ed.* **1999**, *38*, 3165.
- 11 Hagrman, D.; Warren, C. J.; Haushalter, R. C.; Rarig, R. S. Jr.; Johnson, K. M. III; LaDuca, R. L. Jr.; Zubieta, J. *Chem. Mater.* **1998**, *10*, 3294.
- 12 Pope, M. T. *Heteropoly and Isopoly oxometalates*, Springer, New York, **1983**.
- 13 Inoue, M.; Yamase, T. *Bull. Chem. Soc. Jpn.* **1995**, *68*, 3055.
- 14 Fuchs, J.; Hartl, H. *Angew. Chem., Int. Ed. Engl.* **1976**, *15*, 375.
- 15 Howarth, O. W.; Kelly, P.; Petersson, L. *J. Chem. Soc., Dalton Trans.* **1990**, 81.
- 16 Niven, M. L.; Cruywagen, J. J.; Heyns, J. B. B. *J. Chem. Soc., Dalton Trans.* **1991**, 2007.
- 17 Hagrman, D.; Hagrman, P.; Zubieta, J. *Inorg. Chim. Acta* **2000**, 300-302, 212.
- 18 Xi, R.; Wang, B.; Isobe, K.; Nishioka, T.; Toriumi, K.; Ozawa, Y. *Inorg. Chem.* **1994**, *33*, 833.
- 19 Xu, J.-Q.; Wang, R.-Z.; Yang, G.-Y.; Xing, Y.-H.; Li, D.-M.; Bu, W.-M.; Ye, L.; Fan, Y.-G.; Yang, G.-Y.; Xing, Y.; Lin, Y.-H.; Jia, H.-Q. *Chem. Commun.* **1999**, 983.
- 20 Hagrman, D.; Zubieta, C.; Rose, D. J.; Zubieta, J.; Haushalter, R. C. *Angew. Chem., Int. Ed. Engl.* **1997**, *36*, 795.
- 21 Hagrman, D.; Sangregorio, C.; O'Connor, C. J.; Zubieta, J. *Chem. Commun.* **1998**, 1283.
- 22 Hagrman, D.; Sangregorio, C.; O'Connor, C. J.; Zubieta, J. *J. Chem. Soc. Dalton Trans.* **1998**, 3707.
- 23 Hagrman, D.; Zubieta, C.; Rose, D. J.; Zubieta, J.; Haushalter, R. C. *Angew. Chem., Int. Ed. Engl.* **1997**, *36*, 873.
- 24 Hagrman, P. J.; Zubieta, J. *Inorg. Chem.* **1999**, *38*, 4480.
- 25 Zapf, P. J.; Warren, C. J.; Haushalter, R. C.; Zubieta, J. *Chem. Commun.* **1997**, 1543.
- 26 Wang, R.-Z.; Xu, J.-Q.; Yang, G.-Y.; Bu, W.-M.; Xing, Y.-H.; Li, D.-M.; Liu, S.-Q.; Ye, L.; Fan, Y.-G. *Polyhedron* **1999**, *18*, 2971.
- 27 Debord, J. R. D.; Haushalter, R. C.; Meyer, L. M.; Rose, D. J.; Zapf, P. J.; Zubieta, J. *Inorg. Chim. Acta* **1997**, *256*, 165.
- 28 Gouzerh, P.; Proust, A. *Chem. Rev.* **1998**, *98*, 77.
- 29 Day, V. W.; Fredrich, M. F.; Klemperer, W. G.; Shum, W. *J. Am. Chem. Soc.* **1977**, *99*, 952.
- 30 DasGupta, B.; Katz, C.; Israel, T.; Watson, M.; Zompa, L. J. *Inorg. Chim. Acta* **1999**, *292*, 172.
- 31 Himeno, S.; Niiya, H.; Ueda, T. *Bull. Chem. Soc. Jpn.* **1997**, *70*, 631.
- 32 Román, R.; Gutiérrez-Zorrilia, J. M.; Esteban-Calderón, C.; Martínez-Ripoli, M.; García-Blanco, S. *Polyhedron* **1985**, *4*, 1043.

(E0104039 LI, L. T.; DONG, L. J.)